Charge transfer dynamics in advanced conjugated systems

Pavelyev, Vladislav

Chapter 3

Ultrafast Spectroscopy of Push-Pull Polymers

Modern push-pull polymers for organic photovoltaic are designed on basis of alternating donor and acceptor units. One of the characteristic features of these polymers is the formation of an intramolecular (intrapolymer) ground-state charge transfer complex (CTC) which brings enhanced absorption in the red region of the solar spectrum. Despite impressive efficiencies demonstrated with devices based on the push-pull polymers, still very little is known about the initial steps of charge generation which are crucial for photon-to-voltage conversion efficiencies. In this chapter, Photo Induced Absorption (PIA) spectroscopy is used to study charge separation dynamics in two push-pull polymers: poly[*N*-9″-heptadecanyl-2,7-carbazole-*alt*-5,5-(4′,7′-di-2-thienyl-2′,1′,3′-benzothiadiazole)] (PCDTBT) and benzo-[1,2-b:3,4-b′:5,6-d″] trithiophene-diketopyrrolopyrrole (BTT-DPP) and their blends with the phenyl-C71-butyric-acid-methyl ester ([70]PCBM) acceptor. We demonstrate the interplay between the intra- and inter- molecular charge separation processes by making use of blends with different acceptor concentration. It is shown that for a push-pull polymer to be efficient, a faster-than-10-ps channel should be opened for the electron to escape the polymer to [70]PCBM and thereby avoid geminate recombination.

The current chapter is based on the following publication:
Kozlov, O.; de Gier, H. D.; Pavelyev, V. G.; van Loosdrecht, P. H. M.; Havenith, R. W. A.; Pshenichnikov, M. S., Charge Transfer Pathways in Blends of Push-Pull Polymers with [70]PCBM. *in preparation(2015)*.

3.1. Introduction

Bulk heterojunction solar cells are one of the promising classes of Organic Photovoltaics (OPVs) technologies. Nowadays these devices attract a lot of attention[1,2] due to their promising power conversion efficiencies (PCE), which recently reached more than 10%[3], and their potentially low-cost production.

The active layer in a solution-processed solar cell consists of the electron donating unit and electron accepting unit. If the role of the acceptor is conventially taken up by [60]PCBM or [70]PCBM – soluble derivatives of the C60 or C70 fullerenes[4-7], the role of the donor has recently been changed from conventional semiconducting polymers[8] to the so-called push-pull polymers[2]. The push-pull polymers are based on alternating donor and acceptor units which gives them a unique property: an ability to form an intramolecular ground-state CTC[9] with a narrowed band gap and an increased absorption in the red part of the solar spectrum.

One of the first reviews on the tools to manipulate and optimize the band gap of conjugated polymers for OPVs was published by van Mullekom *et al*.[10] The authors showed that one of the most successful approaches to narrow the band gap and hence to extend the absorption in IR is the manipulation of the donor:acceptor repeating units in co-polymer. Furthermore, they presented a study of a series of alternating donor-acceptor materials, which demonstrated one of the smallest band gaps (~0.3 eV) and revealed the achievable limits of the corresponding co-polymers. Moreover, it was shown that the influence of side-chains, main chain conformation, and mesoscopic order may give rise to additional effects on the band gap; however, these effects were not fully elucidated.

Recent developments of push-pull polymers for bulk heterojunction photovoltaics have been thoroughly described in another review by Yong Cao *et al*.[9] The authors described the proper choice of the donor and acceptor units within the push-pull polymer and compared a large set of modern donor and acceptor moieties and their combinations. The authors also reviewed new perspective strategies for the push-pull conjugated photovoltaic materials. One of the possible ways is to better align the energy levels of the donor and acceptor species through the interaction of the *d*-orbitals of the metal (platinum for instance) with the ligand orbitals. Another perspective approach is to use a new molecular design strategy, the so-called pended push-pull conjugated polymer for the OPV applications. The

main difference (as compared to the ordinary polymerization approach) is to construct the main polymer chain from the electron-rich units, while the electron-withdrawing units are attached onto the end of the side chains and connected to the main chain through a π-bridge. Such design poses several advantages. First, these two-dimensional structures provide a good solubility and better isotropic charge transporting properties, as compared to their linear counterparts. Second, due to the post-functionalization approach, the molecular weight and the degree of polymerization are well controlled.

Continuing on the issue of effects of the polymer structure on its photophysical properties, Tautz *et al.*[11] applied time–resolved PIA spectroscopy to study charge generation and recombination processes in the low band gap co-polymers. The authors examined the charge generation properties in thin films of a set of co-polymers (PCPDT-BDT, PCPDT-BT, PCPDT-2TTP, PCPDT-2TBT) that differ by the donor:acceptor moieties and spacer, and compared these co-polymers with the well-studied homopolymer P3HT. The obtained results demonstrated that co-polymers with a strong acceptor unit show large yields of polaron formation (up to 24% in PCPDT-BDT) as compared to much lower value for the homopolymer P3HT (~8%). Furthermore, it was found that elongation of the π-conjugated spacers in between the donor and acceptor moieties tend to increase the charge recombination time. Another interesting aspect was the influence of the electron affinity (EA) of the acceptor on the recombination lifetime within one topological category. In general, the authors noted that the higher the EA of the acceptor, the shorter the recombination time, in full accord with our observations in Chapter 2. Unfortunately, the authors did not attempt to study bulk heterojunctions of the co-polymers with an external acceptor, such as [60]PCBM or [70]PCBM, which would have borne more resemblance to the real OPV devices.

Bakulin *et al.*[1,12] have taken another approach to studying ultrafast photophysics by a novel IR pump-push photocurrent (PPP) spectroscopy technique in a variety of donor:acceptor systems like the MDMO-PPV:[70]PCBM, PCPDTBT:[70]PCBM[13], and BTT-DPP. The selected polymers differ by the position of the LUMO levels and hence the driving energy for the electron transfer (ET). The latest polymer nicely complement the series as it was shown to have too small offset between the LUMO levels with [70]PCBM to ensure the ET.[14] The authors demonstrated that the charge transfer (CT) states generated through both ET and HT channels are almost identical. This conclusion was based on a fact that PPP recombination

dynamics for both channels are very similar. Secondly, Bakulin *et al.* showed that the efficiency of generating bound CT states increases with the decrease of the energy difference between donor and acceptors LUMO energy levels. A possible explanation for such behavior is that a larger energy difference leads to a larger excess energy, which results in the decreased probability of the CT states formation. Important as they are, the studies by Bakulin *et al.* were focused on pushing the CT states by IR light without addressing much the pathways to and escape routes from the CT states. Furthermore, the very nature of CT states as intra- (i.e. within the polymer) or inter- (i.e. between the polymer and fullerene) molecular remained unclear as well as their interplay during the charge generation and separation processes.

In this chapter we report on a study of the intricate interplay between the intra- and inter- molecular CT processes following photon absorption. To distinguish between the two processes, blends with two different donor:acceptor LUMO energy level offsets were used. First, a PCDTBT:[70]PCBM combination that was used in efficient collar cells by Park and co-workers[13], exhibits a high LUMO energy offset of ~0.4 eV[15]. Second, a BTT-DPP:[70]PCBM blend with the BTT-DPP polymer synthesised by the group of McCulloch (Imperial College, UK), possesses almost zero (~0.2 eV) LUMO energy offset but is quite efficient (~3% solar cell efficiency[14]) via the HT process. To reveal the charge dynamics we used an ultrafast PIA spectroscopy. PIA anisotropy has been analysed to assist in the separation of the ET and HT channels for charge production. Our studies demonstrate that efficient charge generation (with a minimum geminate recombination) in a push-pull polymer can be reached only if a faster-than-10-ps channel will be opened for the electron to escape the polymer to [70]PCBM.

3.2. Experimental section

3.2.1. Materials

The PCDTBT polymer was obtained from 1-Material company, while [70]PCBM was purchased from Solenne B.V. BTT-DPP polymer was obtained from the group of J. Durrant (Imperial College, UK), and was synthesised in the group of I. McCulloch (Imperial College, UK). All materials were dissolved separately in orthodichlorobenzene (ODCB) at a concentration of 25 g/l that was chosen to

optimize the OD of the samples. Separated solutions were stirred for 12 hours at ~50°C. Blends were prepared by mixing the solutions of the polymers and [70]PCBM. The weight ratios from 1:0 to 1:4 were used to determine the optimal (from charge photogeneration's point of view) concentration of the acceptor in the blend. Solutions of the mixtures were steered again for 12 hours at ~50°C. Films were prepared on microscopic cover slides (22x22 mm, 150 μm thickness) by spin coating at 1000 rpm in the air atmosphere of 30 μl of the mixture per film. During spin-coating the volume of the film covered evenly all surface of the slide. After spin-coating the films were dried under the air atmosphere during 6 hours.

3.2.2. Steady-state absorption spectroscopy section

Absorption spectra of the used materials were recorded with a Perkin-Elmer Lambda 900 spectrometer.

3.2.3. Ultrafast experiment section

To monitor the dynamics of photogenerated charges in the samples we apply a PIA technique, which allows obtaining the evolution of the photoinduced charge density in time with sub-100 fs resolution. The principles of this technique together with experimental details have been already described in the previous chapters (see Chapter 1, 2).

The polaron absorption spectra were obtained using a different setup based on two commercial optical parametrical amplifiers (TOPAS) from Light Conversion which operated in the visible (500-700 nm, as a pump) and IR (1.2-20 μm, as a probe) regions. The TOPASes were seeded by a Hurricane Ti:Sapphire regenerative amplifier (Spectra Physics). The time resolution varied with the probe wavelength but did not exceed ~500 fs in all cases.

3.3. Results and Discussion.

3.3.1. Structure of studied materials and linear absorption spectra

Figure 3.1 shows chemical structures of the studied materials and energy levels of the frontier molecular orbitals.[15-17] In the PCDTBT and [70]PCBM pair, the energy offset between the LUMO levels is ~0.4 eV which is sufficient for ET from the

donor to the acceptor. In contrast, for the BTT-DPP and [70]PCBM combination, the LUMO-LUMO offset does not exceed 0.2 eV which might not be enough for splitting the polymer exciton into charges.

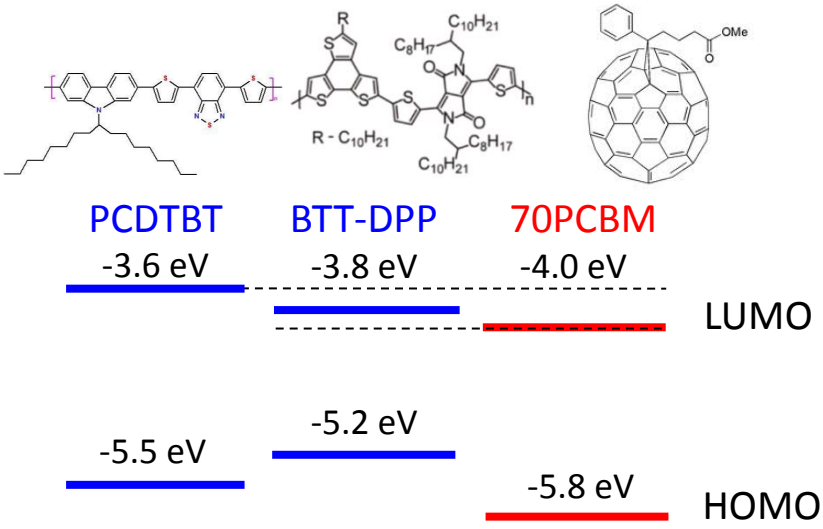

Figure 3.1. *Chemical and simplified electronic structure of the studied materials (above) with the positions of the HOMO and LUMO levels[16-18] (below). HOMO and LUMO denote the highest occupied molecular orbital and the lowest unoccupied molecular orbital, respectively.*

Absorption spectra of the studied samples are depicted in Figure 3.2. The two polymers show different band gaps which are mainly determined by the position of the energy levels of the donor and acceptor moieties within the polymer.[10] For instance, PCDTBT has a maximum absorption at 560 nm and a band gap of 1.9 eV; BTT-DPP has a maximum absorption at 760 nm and a lower band gap of 1.4 eV.

To reveal absorptions of the polymer and the fullerene components in the blend (which could deviate from 1:1) we perform a tentative decomposition of the blend absorption spectrum. The decomposition was obtained as the weighted sum of the polymer and the fullerene contributions until the blend absorption spectrum is best reproduced. The resulted spectra are close to the measured absorption of the blends although with some notable deviations in the red region (see the yellow curves in Fig. 3.2).

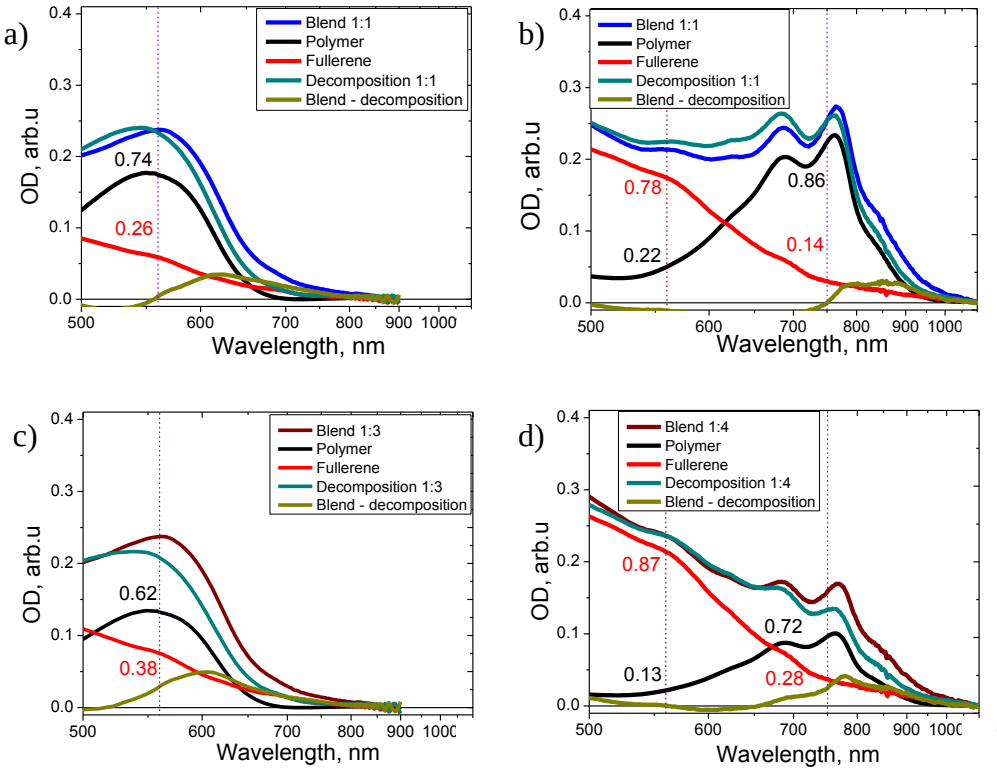

Figure 3.2. *Absorption spectra (scaled according to decomposition coefficient) of the PCDTBT (a,c) and BTT-DPP (b,d) blends for different concentrations (shown in the legends) together with their decomposition into the polymer and [70]PCBM spectra. The black and red numbers represent shares in absorption of the polymer and fullerene, respectively at the excitation wavelength shown by the dotted line (two lines in case of BTT-DPP). The difference between the spectra of measured absorption of the blend and its decomposition is presented by yellow curves.*

In both cases this inconsistency could be explained as a consequence of existence of the interactions between the donor and acceptor molecules in the blend, i.e. by the formation of the ground state CTC[19] (Chapter 2). For PIA spectroscopy, we used excitation wavelengths close to the absorption maxima: 560 nm for the PCDTBT-based blends and 750 nm for the BTT-DPP-based blends. In the latter case, 560 nm excitation wavelength was also used to vary the partition between BTT-DPP and [70]PCBM absorptions.

3.3.2. IR and polaron absorption spectra

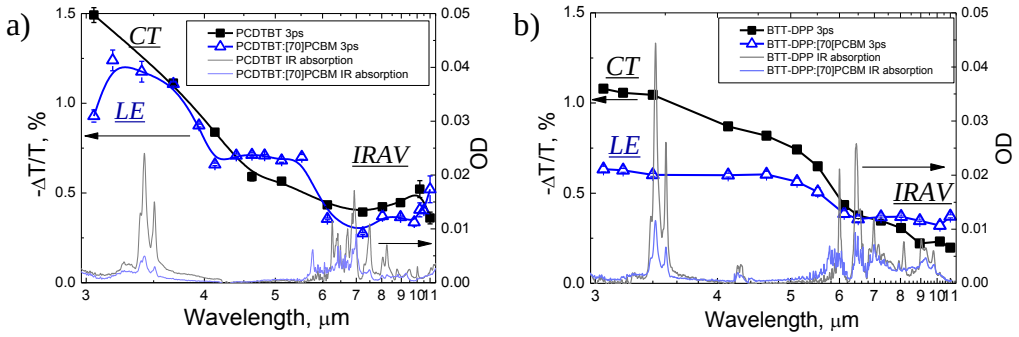

Figure 3.3. *PIA (symbols) and IR absorption (thin lines) spectra of the PCDTBT (a) and BTT-DPP (b) based films for excitation wavelengths of 560 nm and 750 nm, respectively. Spectra for the neat polymer depicted in black, for the 1:1 blend – in blue. The delay between the excitation and probe pulses is set at 3 ps. CT, LE and IRAV mark the IR absorption bands and stands for charge transfer excitons, low energy polaron band, and IR active vibrations, respectively.*

In Figure 3.3, IR absorption spectra of the studied materials are shown. The IR absorption spectra of the neat materials and blends with [70]PCBM closely follow each other for both polymers. The most noticeable difference is the existence of the additional peak at ~5.8 μm in the spectra of the blends with [70]PCBM. This peak was attributed to the carbonyl (C=O) stretch mode of the [70]PCBM molecule.[20] The next feature is different optical density (mostly around 3.5 μm and in the region of 6-9 μm, where different C-H modes of the polymer absorb) of the neat materials in comparison to blends. Such a difference could be explained by a thinner film of the blend with [70]PCBM due to different viscosity of the solution from which the film was spin-cast.

All PIA spectra demonstrate similar features: a well pronounced broadband peak extending from ~3 to ~7 μm. For semiconducting polymers, this feature was assigned[21] to the low-energy (LE) polaron (for the blend) and charge-transfer (CT) exciton (for the neat polymers) absorption.[22] Since the films are transparent around 3 μm (except readily avoidable CH-stretch lines around ~3.3 μm) this wavelength suits well for the probe pulse as it allows for background-free measurements.

3.3.3. PIA dynamics

Figure 3.4 shows isotropic transients for PCDTBT- and BTT-DPP-based films with different concentration of [70]PCBM. The experimental data were fitted with a tri-exponential function:

$$\Delta T_{ISO} = A_0 + A_1 \exp(-t/\tau_1) + A_2 \exp(-t/\tau_2) - A_3 \exp(-t/\tau_3) \quad (2)$$

convoluted with a Gaussian apparatus function (standard deviation σ~50 fs). Here, A_i and τ_i stand for amplitudes and times, respectively, of the exponential function, while A_0 stands for the offset. The fit parameters for the materials measured in blends are given in Table 3.1.

The PIA results for PCDTBT films (Fig.3.4a) demonstrate that recombination dynamics in the pristine polymer are fast and show very minor contribution of long-lived charges. Indeed, large energy offset between the polymer species accelerate the recombination. Hence we conclude that the intramolecular recombination within the polymer occurs at a ~100 ps timescale (Table 3.1).

The situation changes after addition [70]PCBM to the blend. First of all, this leads to increase of the yield of the initially produced charges (higher initial amplitude of the PIA transient), which reaches its maximum at 1:3 donor:acceptor concentration. Furthermore, there is a 5-fold increase as compared to the neat polymer of the long-time offset or, in other words, in long-lived charges. This fact means that after adding the acceptor to the blend, the charges are transferred from the polymer to [70]PCBM and escape the intrapolymer recombination process.

Finally, after adding [70]PCBM the ingrowing response sets up with a timescale of ~2 ps. Such a growing behaviour is consistent with excitation of the [70]PCBM molecules in the fullerene domain away from the donor and acceptor interface. In this case, the created excitons need some time to reach the polymer and fullerene interface and contribute to the charge separation via the HT process.[23] This conclusion is strengthened by the fact that the contribution of the ingrowing component increases with the increase of [70]PCBM concentration (compare blue and brown curves in Fig.3.4b) as the [70]PCBM absorption share at the excitation wavelength of 560 nm increases (Fig.3.2a-c).

Therefore, the PCDTBT-based blends demonstrate both ET and HT channels of charge generation via the polymer and fullerene excitations, respectively. The contribution of the HT process remains relatively low (estimated as ~30%) as dictated by the contrast between the polymer and fullerene linear absorption at the

excitation wavelength (Fig. 3.2a-c). Overall, in the 1:3 blend there remain about 50% of the initially photogenerated charges, in a sharp contrast to the neat polymer where most charges recombine on a 100-ps timescale.

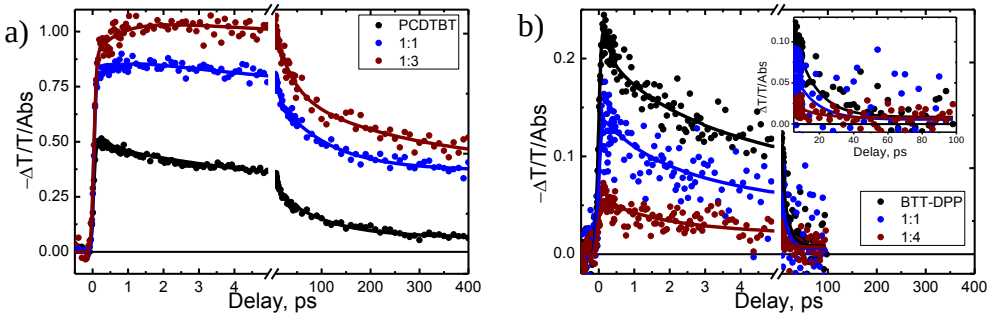

Figure 3.4. *Isotropic transients at the excitation wavelength of 560 nm for PCDTBT (a) and 750 nm for BTT-DPP (b) blends with different polymer:fullerene content (shown in the legends). All transients are normalized to film absorption (i.e. to the number of absorbed photons) to allow direct comparison of different concentrations. Note the breaking point at the delay axis. The inset in Fig. 3.4b demonstrates a weak offset at long delays after 750 nm excitation of BTT-DPP mixtures.*

Figure 3.4b shows PIA transients for the BTT-DPP blends. The first striking feature is their identical shape irrespective [70]PCBM concentration. This is confirmed by fitting of the transients with a bi-exponential function: the identical timescales of ~15 ps point to highly efficient intrapolymer recombination of the CT exciton, with barely existent ET to [70]PCBM. This is in agreement with previous studies by Bakulin *et al.*[12], where they concluded that this is due to insufficient LUMO-LUMO offset between BTT-DPP and [70]PCBM (see Fig.3.1).

Another noticeable feature of the BTT-DPP-related transients is that their initial amplitude decreases with the increase of [70]PCBM content. Note that the transients are normalized on the number of photons absorbed so that possible decrease of film absorption can be safely ruled out. Also, [70]PCBM almost does not absorb at the excitation wavelength of 750 nm (Fig.3.2b,d); therefore, differences in partial absorptions cannot be an explanation either. At this point we could only speculate that such a decrease of the signal is caused by the CT excitonic response that contributes to the overall response (see Figure 3.5) at the

probe wavelength of 3 μm. Alternatively, the absorption cross-section at 3 μm of the CT state (that is probed in the push experiment[1,12]) might be higher than the polaron absorption cross-section. Verifying these hypotheses would require additional measurements at a different probe wavelength.

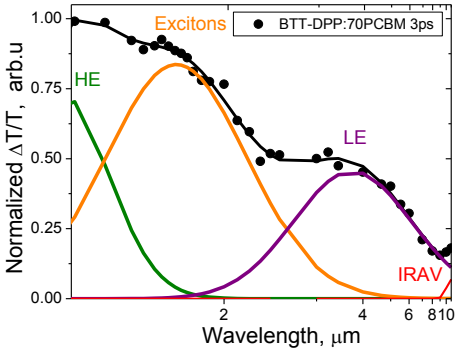

Figure 3.5. *Polaron spectrum of BTT-DPP:[70]PCBM blend for 1:1 concentration together with its provisional decomposition into three Gaussian peaks. The excitation wavelength is 525 nm.*

Table 3.1. *Fitting parameters of the studied blends transient spectra @560nm and @750 nm for PCDTBT and BTT-DPP, respectively.*

Material	Isotropic decay fit parameters			
	A_1 (τ_1)	A_2 (τ_2)	Ingrowing time τ_3, ps	Offset
PCDTBT neat	0.4 (5ps)	0.45 (100ps)	0	0.07
PCDTBT 1:1	0.2 (5ps)	0.35 (100ps)	0.5	0.45
PCDTBT 1:3	0.18 (5ps)	0.32 (100ps)	2	0.5
BTT-DPP neat	0.25 (2ps)	0.72 (15ps)	0	0.03
BTT-DPP 1:1	0.2 (2ps)	0.54 (15ps)	0	0.26
BTT-DPP 1:4	0.1 (2ps)	0.6 (15ps)	0	0.3

From the 750 nm excitation experiment we concluded that there are no signatures of long-lived ET in BTT-DPP-based blends, in sharp contrast to the PCDTBT-based blends. Extremely low [70]PCBM absorption at this wavelength (Fig. 3.2) does not allow studying the HT process, so that similar transients were collected at the 560 nm excitation wavelength (Fig. 3.6), where fullerene absorption dominates over the polymer one.

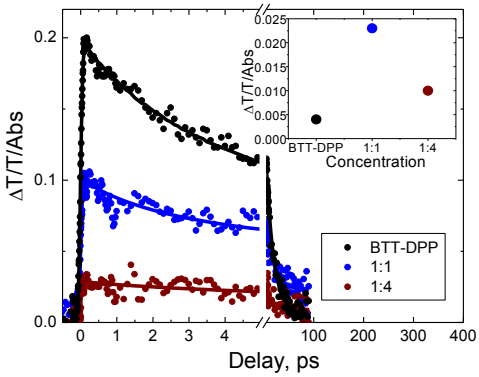

Figure 3.6. *Isotropic transients at excitation wavelength of 560 nm for BTT-DPP blends (normalized to film absorption) with different polymer:fullerene content (shown in the legend). Dots represent measured data, lines are the fits; fit parameters are given in Table 3.2. The inset shows the long-time (90 ps) amplitude as a function of the [70]PCBM content.*

The transients are found to be similar to the 750 nm excitation dynamics at the time scale of 15 ps. However, at long delays the transients are remarkably different: while absorption in pristine BTT-DPP approaches zero, the blends with [70]PCBM result in a noticeable offset. The 1:1 blend shows the highest share of the separated charges at 90 ps, even higher than for the 1:4 blend. This trend is consistent with the HT process as there is a trade-off between the amount of fullerene (the HT contribution increases) and the size of fullerene domains (the excitons formed deeply in the [70]PCBM domain cannot reach the interface). An acceptor content of ~1:1 appears to be optimal for charge separation. Nonetheless, even at this optimal concentration only a small fraction of ~5% of the initially generated charges survives by 100 ps. Therefore, in the BTT-DPP:[70]PCBM blends at the short excitation wavelength the charge generation occurs via the HT process, however, with low efficiency.[24]

The intrapolymer recombination dynamics in pristine polymers occur on a 15 ps (BTT-DPP) and 100 ps (PCDTBT) timescale with no surviving long-lived charges. As we know from Chapter 2, the higher recombination rate corresponds to higher EA of the acceptor (see Fig. 2.5 in Chapter 2). The latter also results in a pronounced red shift of absorption due to narrowed band gap (see Fig. 2.3 in Chapter 2). Therefore, both features observed in the polymers are consistent with

the trends observed for fluorine acceptors. The closest ones to BTT-DPP by EA, DNFon (-3.7 eV) and TNFon (-3.96 eV), exhibit similar recombination times of 20 ps and 7 ps, respectively. Their absorption also extends beyond 700 nm. This proves the prediction made in Chapter 2 that the two opposite trends - higher acceptor EA increases the driving force for charge separation but also inevitably increases the rate of undesirable charge recombination – should be carefully counterbalanced in designing novel polymer:fullerene bulk heterojunctions.

Table 3.2. *Fitting parameters of the studied blends transient spectra @560nm for BTT-DPP.*

Material	Isotropic decay fit parameters			
	$A_1(\tau_1)$	$A_2(\tau_2)$	Ingrowing time τ_3, ps	Offset
BTT-DPP neat	0.26 (2 ps)	0.7 (15 ps)	0	0.04
BTT-DPP 1:1	0.16 (2 ps)	0.46 (15 ps)	0	0.38
BTT-DPP 1:4	0.08 (2 ps)	0.58 (15 ps)	0	0.34

Summarizing the experiment discussed insofar: blends with large LUMO-LUMO offset (the case of PCDTBT) show a 5-fold increase of the long-lived charges as compared to the neat polymer. This result points at the efficient intermolecular charge separation in the PCDTBT blends driven by the ~0.4 eV LUMO-LUMO offset (ET) and ~0.3 eV HOMO-HOMO offset (HT). In contrast, the ~0.2 eV LUMO-LUMO offset in the case of BTT-DPP does not allow for any significant ET process. The only long-lived charges originate from the fullerene excitation followed by the HT process (the HOMO-HOMO offset of ~0.6 eV).

3.3.4. Excitation spectra

To strengthen the conclusions of the previous Section, we measured the action (excitation) spectra of both materials, i.e. the PIA responses over a range of excitation wavelengths – ~515 nm, 560 nm, 600 nm, 640 nm, 670 nm, ~710 nm, 750 nm and ~800 nm (Figure 3.7). For comparison, absorption spectra are plotted in the same graph (solid lines).

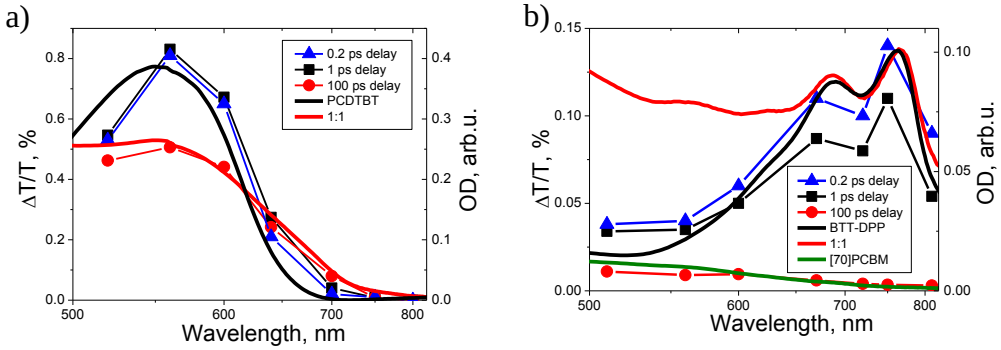

Figure 3.7. *Comparison of the excitation (symbols) and absorption spectra (arbitrarily scaled, thick lines) for 1:1 PCDTBT:[70]PCBM blend (a) and 1:1 BTT-DPP:[70]PCBM blend (b) at delays of 1 ps (black) and 100 ps (red). The absorption spectra are shown to highlight their overlap with the excitation spectra.*

For the PCDTBT:[70]PCBM blend, the short-time response lays in between the polymer and blend absorption spectra (Fig. 3.7a, blue and black symbols). This confirms the previous finding that on the short time scale the photoinduced signal originates mostly from the ET process but has some (interfacial) contribution from the HT process. The long-time excitation spectrum (Fig. 3.7a, red symbols) closely follows the absorption of the blend, which confirms the dual – ET and HT related - origin of the signal. At the long wavelengths (around 700 nm) the contribution from [70]PCBM excitation (and hence a HT) dominates due to its higher absorption as compared to the polymer (see Fig. 3.2). Hence, our previous conclusion that in the PCDTBT:[70]PCBM blends both processes, ET and HT, complement each other, receives an additional proof. The two processes acting in unison result in a high power conversion efficiency demonstrated by devices based on the PCDTBT polymer.

The excitation spectrum of the BTT-DPP:[70]PCBM blend exhibits a totally different behaviour. The short-time response closely follows the polymer absorption spectrum (Fig. 3.7b, blue and black curves) rather than the blend absorption, especially at the short wavelengths. This means that at short times the PIA signal originates mainly from the CT excitons (i.e. polymer excitation). However, the long-time excitation spectrum has nothing in common with neither

blend nor polymer absorption spectra but is more consistent with the fullerene absorption spectrum. This convincingly demonstrates that at long times when the contribution for the CT (intrapolymer) excitons fully vanishes, the contribution of the HT process dominates.

3.3.5. PIA anisotropy dynamics

Together with PIA isotropic transients, the anisotropy dynamics were also obtained, which are useful in the separation of the two channels for charge production: ET and HT.[23] When a push-pull polymer absorbs light, the electron and hole become separated which results in a CT exciton. Its transient dipole moment is preferentially oriented along the polarization of the excitation pulse which leads to high anisotropy values. In contrast, when the fullerene is photoexcited, the transient dipole moment of the resulted polaron absorption at the polymer site has no memory for the polarization of the excitation pulse due to isotropic nature of HT. Therefore, for the HT process the anisotropy value is close to zero.[23] This provides a convenient contrast parameter to distinguish between the ET and HT processes.

Figure 3.8 shows the transient PIA anisotropy of the studied materials.

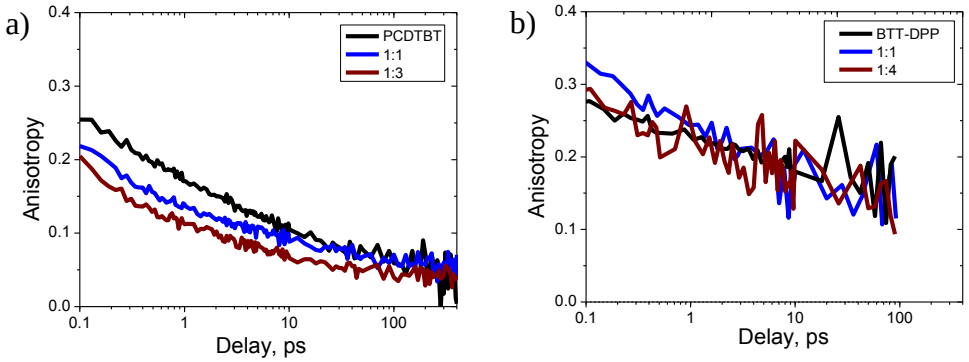

Figure 3.8. *Anisotropy transients for PCDTBT:[70]PCBM blends at 560 nm excitation (a) and BTT-DPP:[70]PCBM blends at 750 nm excitation (b). The blend composition is shown in the legend.*

The high values of initial anisotropy are in line with the fact that most of the PIA signal originates from the polymer excitation. At longer times, the anisotropy decreases for all samples albeit to the different extent. The most probable reason for such loss of the transient dipole moment orientation of the polaron (CT exciton) is hopping from one polymer segment to another with a different orientation of the transient dipole moment.

For the PCDTBT-based blends (Fig. 3.8a), the value of initial anisotropy slightly decreases (from 0.25 to 0.2) with increase of the [70]PCBM content. This decrease signifies increased contribution of the excitons in the [70]PCBM domains with zero anisotropy. Furthermore, the anisotropy decays with time from initial values of 0.2-0.25 to ~0.05 at 100 ps (i.e. by a factor of 4-5) and keeps on decreasing. Therefore, CT excitons and/or polarons are quite mobile that they are free to move away from the place they were created. This is reminiscent to the anisotropy behaviour for relatively weak fluorine acceptors such as 4CN-NFon (Chapter 2, Fig. 2.6 and Fig. 2.7a).

Figure 3.8b shows anisotropy dynamics for the BTT-DPP-based blends which is distinctly different from those for the PCDTBT case. First, the initial value of anisotropy almost does not change with addition of [70]PCBM. Secondly, at 100 ps the anisotropy decreases only by a factor of 2 which points to the reduced mobility of the CT excitons/polarons. This can be understood as follows: because the ET to the [70]PCBM is hindered by an unfavourable LUMO-LUMO offset, the true polaron (i.e. the electron at the [70]PCBM and the hole at the polymer) is not formed. Instead, a bound intrapolymer hole-electron pair, i.e. a CT exciton, is created. Although both the electron and the hole are delocalized along the acceptor-donor moieties of the polymer, their mutual attraction does not allow them to become really mobile which results in high anisotropy. This is quite similar to the localization of the polarons in the blends with the higher EA fluorine acceptors (Chapter 2, Fig. 2.6).

Figure 3.9 shows anisotropy excitation spectra of the PCDTBT:[70]PCBM and BTT-DPP:[70]PCBM blends with 1:1 weight ratio. In the PCDTBT:[70]PCBM case, the anisotropy is fairly constant at all excitation frequencies and times. Only at 560 nm the anisotropy becomes slightly lower, most probably, because of the increased [70]PCBM contribution, in full agreement with our previous conclusions (Fig. 3.7a).

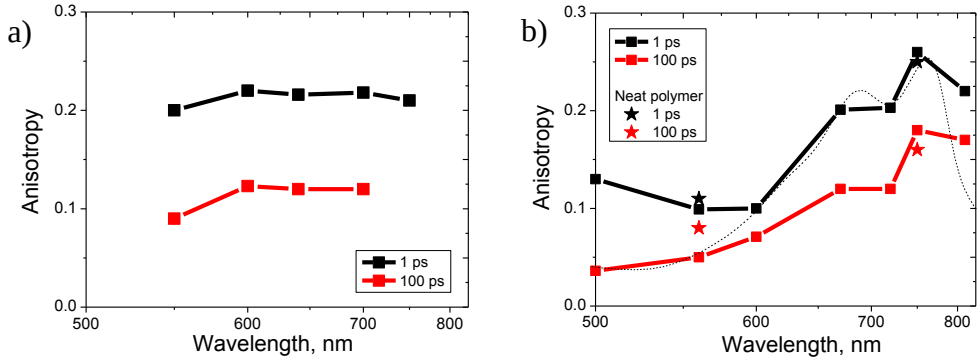

Figure 3.9. *Comparison of the anisotropy excitation spectra of PCDTBT:[70]PCBM (a) and BTT-DPP:[70]PCBM (b) blends with 1:1 weight ratio. The stars in (b) show anisotropy of the neat polymer at two wavelengths for 1 ps (black) and 100 ps (red) delays. The dashed curve represents a scaled (in a way to provide the best visual overlap with the anisotropy excitation spectrum at 1 ps) absorption spectrum of the polymer for comparison.*

A more intriguing anisotropy spectrum is demonstrated by the BTT-DPP:[70]PCBM blend which shows a strong spectral response (Fig. 3.9b). The short-time anisotropy mostly follows the polymer absorption spectrum because of the prevalence of CT excitons originated from the polymer excitation. This is in agreement with our PIA data and is also confirmed by independent measurements on the neat polymer film at two excitation wavelengths (Fig. 3.9b, black stars). As the anisotropy reflects the mutual orientation of the directions of the transient dipole moments in the visible and IR regions, these orientations possess more angular inhomogeneity at shorter wavelengths. Such spectral dependence of the anisotropy is not very common because the vibronic structure does not typically lead to different transient dipoles orientations (compare, for instance, with Fig. 3.9a). Therefore, we speculate that anisotropy decrease at the short wavelengths is due to the second, higher energy CT band with a lower and differently-angled transient dipole moment.

At long delays (red squares) and long wavelengths, the anisotropy decreases by only approximately a third from its initial value while the isotropic PIA signal decreases by a factor of 25 at 750 nm (Fig. 3.7b). At the shorter wavelengths, the anisotropy decays by a factor of 2 to the value of ~0.05, while the neat-polymer anisotropy hits to ~0.08. Therefore, at these wavelengths and times the ET

contribution to the anisotropy is largely overwhelmed by the HT contribution for which anisotropy should be close to zero.

Our findings on the anisotropy wavelength dependence of films of BTT-DPP are in agreement with previous studies performed by Bakulin *et al.*[12] based on current detection (the so-called push technique[25]). For instance, at the excitation wavelength of 700 nm relatively high anisotropy of ~0.15 was obtained, while at the 520 nm excitation the anisotropy is close to a half of this value (~0.07). The difference was attributed to the different charge generation pathways. Thus, with the excitation at 700 nm, mostly the donor polymer is excited, which leads to the high value of anisotropy. In the case of 520 nm excitation, mostly acceptor fullerene is excited, and the anisotropy value is low. The anisotropy values obtained by Bakulin *et al.* are almost twice smaller than obtained herein (0.25 and 0.12, respectively). This inconsistency can be explained by different molecular weights of BTT-DPP polymers that significantly change the morphology of the active layer.[24] Based on these observations and taking into account the amplitudes of the PIA transients, Bakulin *et al.* concluded that in the BTT-DPP:[70]PCBM blends the yield of generated CT states is ~10 times higher for the ET than for the HT. Our measurements demonstrate a similar value of ~6. Such a difference between the yields of ET/HT has been attributed to a much smaller LUMO difference between the donor and acceptor as compared to the HOMO-HOMO energy difference.

Therefore, anisotropy data together with the excitation spectrum (Fig. 3.7b) allow us to make the final conclusion. In the BTT-DPP blends the long-lived charges are originating from the HT process at shorter wavelengths, while at longer wavelengths the charges separate within the polymer only, recombine with ~15 ps time. Hence, the anisotropy spectrum appears to be an important argument for such assignments in addition to the excitation spectra. It provides a perfect contrast parameter for discrimination of the polymer and fullerene absorption contributions.

3.4. Conclusions

The ultrafast experiments on two representative push-pull polymers, PCDTBT and BTT-DPP that differ by the donor and acceptor LUMO energy level offsets, demonstrated the intrapolymer charge recombination dynamics at 100 ps and 15 ps time scale, respectively. These dynamics are comparable to those obtained

previously[22,26] in the ground-state CTCs formed between a semiconducting polymer, MEH-PPV, and a series of fluorene electron acceptors. The results clearly indicate that for a push-pull polymer to be efficient, a faster than 10 ps channel should be opened for the electron to escape the polymer to [70]PCBM and thereby avoid geminate recombination.

After addition of the [70]PCBM fullerene to the blend, the interplay between the intra- (i.e. within the polymer) and inter- (i.e. between the polymer and fullerene) molecular charge transfer processes seems to be governed by the value of the LUMO energy offset. Thus, in case of PCDTBT and [70]PCBM blends (where there is a significant LUMO-LUMO offset between the donor and acceptor), both ET and HT channels are equally involved in the light harvesting which makes the blend efficient. In contrast, for the mixtures with a low LUMO-LUMO energy offset (the case of the BTT-DPP polymer and [70]PCBM) the ET is hardly possible, and the HT becomes the only source of the long-lived photogenerated charges. Of course, there is nothing wrong or inefficient about HT *per se*; the problem is that the polymer absorbs a significant amount of the incoming light which is essentially wasted.

3.5. References

1. Dimitrov, S. D.; Durrant, J. R., Materials Design Considerations for Charge Generation in Organic Solar Cells. *Chemistry of Materials* **2013**, *26*, 616-630.
2. Kularatne, R. S.; Magurudeniya, H. D.; Sista, P.; Biewer, M. C.; Stefan, M. C., Donor–Acceptor Semiconducting Polymers for Organic Solar Cells. *Journal of Polymer Science Part A: Polymer Chemistry* **2013**, *51*, 743-768.
3. He, Z. C.; Zhong, C. M.; Su, S. J.; Xu, M.; Wu, H. B.; Cao, Y., Enhanced Power-Conversion Efficiency in Polymer Solar Cells Using an Inverted Device Structure. *Nature Photonics* **2012**, *6*, 591-595.
4. Chang, E. C.; Chao, C.-I.; Lee, R.-H., Enhancing the Efficiency of MEH-PPV and PCBM Based Polymer Solar Cells Via Optimization of Device Configuration and Processing Conditions. *Journal of Applied Polymer Science* **2006**, *101*, 1919-1924.
5. Chen, D.; Nakahara, A.; Wei, D.; Nordlund, D.; Russell, T. P., P3HT/PCBM Bulk Heterojunction Organic Photovoltaics: Correlating Efficiency and Morphology. *Nano Letters* **2010**, *11*, 561-567.
6. Hummelen, J. C.; Knight, B. W.; LePeq, F.; Wudl, F.; Yao, J.; Wilkins, C. L., Preparation and Characterization of Fulleroid and Methanofullerene Derivatives. *The Journal of Organic Chemistry* **1995**, *60*, 532-538.
7. Manca, J. V.; Munters, T.; Martens, T.; Beelen, Z.; Goris, L.; D'Haen, J.; D'Olieslaeger, M.; Lutsen, L.; Vanderzande, D.; De Schepper, L.; Haenen, K.;

Nesladek, M.; Geens, W.; Poortmans, J.; Andriessen, R., State-of-the-Art MDMO-PPV:PCBM Bulk Heterojunction Organic Solar Cells: Materials, Nanomorphology, and Electro-Optical Properties. *Proceedings of the SPIE*, **2003**, *4801*, 15-21.
8. Chiang, C. K.; Fincher, C. R., Jr.; Park, Y. W.; Heeger, A. J.; Shirakawa, H.; Louis, E. J.; Gau, S. C.; MacDiarmid, A. G., Electrical Conductivity in Doped Polyacetylene. *Physical Review Letters* **1978**, *40*, 1472-1472.
9. Duan, C.; Huang, F.; Cao, Y., Recent Development of Push-Pull Conjugated Polymers for Bulk-Heterojunction Photovoltaics: Rational Design and Fine Tailoring of Molecular Structures. *Journal of Materials Chemistry* **2012**, *22*, 10416-10434.
10. van Mullekom, H. A. M.; Vekemans, J. A. J. M.; Havinga, E. E.; Meijer, E. W., Developments in the Chemistry and Band Gap Engineering of Donor–Acceptor Substituted Conjugated Polymers. *Materials Science and Engineering: R: Reports* **2001**, *32*, 1-40.
11. Tautz, R.; Da Como, E.; Limmer, T.; Feldmann, J.; Egelhaaf, H.-J.; von Hauff, E.; Lemaur, V.; Beljonne, D.; Yilmaz, S.; Dumsch, I.; Allard, S.; Scherf, U., Structural Correlations in the Generation of Polaron Pairs in Low-Bandgap Polymers for Photovoltaics. *Nature Communications* **2012**, *3*, 970-970.
12. Bakulin, A. A.; Dimitrov, S. D.; Rao, A.; Chow, P. C. Y.; Nielsen, C. B.; Schroeder, B. C.; McCulloch, I.; Bakker, H. J.; Durrant, J. R.; Friend, R. H., Charge-Transfer State Dynamics Following Hole and Electron Transfer in Organic Photovoltaic Devices. *The Journal of Physical Chemistry Letters* **2012**, *4*, 209-215.
13. Park, S. H.; Roy, A.; Beaupre, S.; Cho, S.; Coates, N.; Moon, J. S.; Moses, D.; Leclerc, M.; Lee, K.; Heeger, A. J., Bulk Heterojunction Solar Cells with Internal Quantum Efficiency Approaching 100%. *Nature Photonics* **2009**, *3*, 297-302.
14. Dimitrov, S. D.; Nielsen, C. B.; Shoaee, S.; Shakya Tuladhar, P.; Du, J.; McCulloch, I.; Durrant, J. R., Efficient Charge Photogeneration by the Dissociation of PC70BM Excitons in Polymer/Fullerene Solar Cells. *The Journal of Physical Chemistry Letters* **2011**, *3*, 140-144.
15. Blouin, N.; Michaud, A.; Gendron, D.; Wakim, S.; Blair, E.; Neagu-Plesu, R.; Belletête, M.; Durocher, G.; Tao, Y.; Leclerc, M., Toward a Rational Design of Poly(2,7-Carbazole) Derivatives for Solar Cells. *Journal of the American Chemical Society* **2007**, *130*, 732-742.
16. Nielsen, C. B.; Ashraf, R. S.; Schroeder, B. C.; D'Angelo, P.; Watkins, S. E.; Song, K.; Anthopoulos, T. D.; McCulloch, I., Random Benzotrithiophene-Based Donor-Acceptor Copolymers for Efficient Organic Photovoltaic Devices. *Chemical Communications* **2012**, *48*, 5832-5834.
17. Ren, G.; Schlenker, C. W.; Ahmed, E.; Subramaniyan, S.; Olthof, S.; Kahn, A.; Ginger, D. S.; Jenekhe, S. A., Photoinduced Hole Transfer Becomes Suppressed with Diminished Driving Force in Polymer-Fullerene Solar Cells While Electron Transfer Remains Active. *Advanced Functional Materials* **2013**, *23*, 1238-1249.

18. Siddiki, M. K.; Li, J.; Galipeau, D.; Qiao, Q., A Review of Polymer Multijunction Solar Cells. *Energy & Environmental Science* **2010**, *3*, 867-883.
19. Zapunidy, S. A.; Martyanov, D. S.; Nechvolodova, E. M.; Tsikalova, M. V.; Novikov, Y. N.; Paraschuk, D. Y., Approaches to Low-Bandgap Polymer Solar Cells: Using Polymer Charge-Transfer Complexes and Fullerene Metallocomplexes. *Pure Appl. Chem.* **2008**, *80*, 2151-2161.
20. Barbour, L. W.; Maureen, H.; Asbury, J. B., Watching Electrons Move in Real Time: Ultrafast Infrared Spectroscopy of a Polymer Blend Photovoltaic Material. *Journal of the American Chemical Society.* **2007**, *129*, 15884–15894.
21. Mizrahi, U.; Shtrichman, I.; Gershoni, D.; Ehrenfreund, E.; Vardeny, Z. V., Picoseconds Time Resolved Photoinduced Absorption by Infrared Active Vibrations as a Probe for Charge Photogeneration in MEH-PPV/C60 Composites. *Synthetic Metals* **1999**, *102*, 1182-1185.
22. Bakulin, A. A.; Martyanov, D. S.; Paraschuk, D. Y.; Pshenichnikov, M. S.; van Loosdrecht, P. H. M., Ultrafast Charge Photogeneration Dynamics in Ground-State Charge-Transfer Complexes Based on Conjugated Polymers. *The Journal of Physical Chemistry B* **2008**, *112*, 13730-13737.
23. Bakulin, A. A.; Hummelen, J. C.; Pshenichnikov, M. S.; van Loosdrecht, P. H. M., Ultrafast Hole-Transfer Dynamics in Polymer/PCBM Bulk Heterojunctions. *Advanced Functional Materials* **2010**, *20*, 1653-1660.
24. Dimitrov, S. D.; Huang, Z.; Deledalle, F.; Nielsen, C. B.; Schroeder, B. C.; Ashraf, R. S.; Shoaee, S.; McCulloch, I.; Durrant, J. R., Towards Optimisation of Photocurrent from Fullerene Excitons in Organic Solar Cells. *Energy & Environmental Science* **2014**, *7*, 1037-1043.
25. Bakulin, A. A.; Rao, A.; Pavelyev, V. G.; van Loosdrecht, P. H. M.; Pshenichnikov, M. S.; Niedzialek, D.; Cornil, J.; Beljonne, D.; Friend, R. H., The Role of Driving Energy and Delocalized States for Charge Separation in Organic Semiconductors. *Science* **2012**, *335*, 1340-1344.
26. Pavelyev, V. G.; Parashchuk, O. D.; Krompiec, M.; Orekhova, T. V.; Perepichka, I. F.; van Loosdrecht, P. H. M.; Paraschuk, D. Y.; Pshenichnikov, M. S., Charge Transfer Dynamics in Donor–Acceptor Complexes between a Conjugated Polymer and Fluorene Acceptors. *The Journal of Physical Chemistry C* **2014**, *118*, 30291-30301.